Diffusion Tensor Registration Using Probability Kernels and Discrete Optimization

Aristeidis Sotiras, Radhouène Neji, J.-F. Deux, Nikos Komodakis, Mezri Maatouk, Alain Rahmouni, Guillaume Bassez, Gilles Fleury, Nikolaos Paragios

INSTITUT NATIONAL DE RECHERCHE EN INFORMATIQUE ET EN AUTOMATIQUE

Diffusion Tensor Registration Using Probability Kernels and Discrete Optimization

Aristeidis Sotiras — Radhouène Neji — Jean-François Deux — Nikos Komodakis — Mezri Maatouk — Alain Rahmouni — Guillaume Bassez — Gilles Fleury — Nikos Paragios

N° 6943

May 2009

Thème BIO

ISSN 0249-6399 ISRN INRIA/RR--6943--FR+ENG

Diffusion Tensor Registration Using Probability Kernels and Discrete Optimization

Aristeidis Sotiras* , Radhouène Neji , Jean-François Deux† , Nikos Komodakis‡ , Mezri Maatouk , Alain Rahmouni , Guillaume Bassez , Gilles Fleury§ , Nikos Paragios

Thème BIO — Systèmes biologiques
Projet Galen

Rapport de recherche n° 6943 — May 2009 — 15 pages

Abstract: In this report, we propose a novel diffusion tensor registration algorithm based on a discrete optimization approach in a Reproducing Kernel Hilbert Space (RKHS) setting. Our approach encodes both the diffusion information and the spatial localization of tensors in a probabilistic framework. The diffusion probabilities are mapped to a RKHS, where we define a registration energy that accounts both for target matching and deformation regularity in both translation and rotation spaces. The six-dimensional deformation space is quantized and discrete energy minimization is performed using efficient linear programming. We show that the algorithm allows for tensor reorientation directly in the optimization framework. Experimental results on a manually annotated dataset of diffusion tensor images of the calf muscle demonstrate the potential of the proposed approach.

Key-words: Registration, DTI, Diffusion tensor, Kernels, Markov Random Fields

* Aristeidis Sotiras, Radhouène Neji and Nikos Paragios are affiliated to Laboratoire MAS, Ecole Centrale Paris, Châtenay-Malabry, France and to Equipe GALEN, INRIA Saclay - Île-de-France, Orsay, France
† Jean-François Deux, Mezri Maatouk, Alain Rahmouni et Guillaume Bassez are affiliated to Centre Hospitalier Universitaire Henri Mondor, Créteil, France
‡ Nikos Komodakis is affiliated to Department of Computer Science, University of Crete, Greece
§ Gilles Fleury is affiliated to Département SSE, Ecole Supérieure d'Electricité, Gif-sur-Yvette, France

Unité de recherche INRIA Futurs
Parc Club Orsay Université, ZAC des Vignes,
4, rue Jacques Monod, 91893 ORSAY Cedex (France)
Téléphone : +33 1 72 92 59 00 — Télécopie : +33 1 60 19 66 08

Recalage d'images IRM de tenseurs de diffusion en utilisant des noyaux de probabilits et un schma d'optimisation discrte

Résumé : Dans ce rapport, nous proposons une nouvelle approche pour le recalage d'images IRM de tenseurs diffusion qui se base sur un schma d'optimisation discrte dans espace de Hilbert. Notre mthode traite aussi bien l'information de diffusion que l'information de localisation spatiale dans un contexte probabiliste. Les probabilits gaussiennes de diffusions sont immerges dans un espace de Hilbert, o nous dfinissons une nergie de recalage qui tient compte la fois de la similarit entre tenseurs et de la rgularit de la dformation dans l'espace des translations et des rotations. L'espace de dformation (six-dimensionnel) est discrtis, ce qui permet d'utiliser une approche efficace de programmation linaire pour optimiser l'nergie dfinie. Nous montrons que l'algorithme permet d'inclure directement la rorientation des tenseurs dans l'tape d'optimisation. Les rsultats exprimentaux sur des images IRM de tenseurs de diffusion du mollet qui ont t pralablement segmentes d'une faon manuelle montrent le potentiel de notre approche.

Mots-clés : Recalage, IRM de diffusion, Tenseur de diffusion, Noyaux, Champs Markoviens Aleatoires

Contents

1 Introduction

1.1 Context and Motivation

Diffusion Tensor Imaging (DTI) is a fairly new modality that is becoming part of many routine clinical protocols due its capability to provide clinicians with detailed information regarding the structure and the geometry of the observed tissues. The acquisition setting allows to compute a field of 3×3 symmetric positive definite matrices that model the uncertainty information (covariance) of a Gaussian distribution over the displacements of water protons in the tissues. DTI has found numerous applications especially in the case of human brain where it has been used to study the connectivity between its different anatomical structures[**?**]. One of the main reasons that DTI has attracted much interest is because of its potential in unveiling the fiber tracts in brain white matter, since diffusive transport in organized tissues is more important along fiber directions and is rather hindered in the orthogonal directions. Lately, efforts have been made to harness the potential of this modality to explore other regions where water diffusion can carry rich information about the architecture of the fibers and the underlying structure and organization. The human skeletal muscles and more specifically the lower leg are of particular interest because they present an ordered structure of elongated myofibers. Moreover, the perspective of studying the effect of neuromuscular diseases (myopathies) on water diffusion in the human skeletal muscle and providing a tool for early diagnosis and quantitative assessment of muscular weakness and atrophy due to illness based on DTI information is enticing. In all the clinical studies in order to assess the evolution of the disease or to compare different patients between them an appropriate step of spatial normalization has to take place. This step is of great importance, as failure to establish valid correspondences will influence the quality of the drawn conclusions.

1.2 Prior Work

Diffusion tensor (DT) registration is an inherently intricate problem because of the directional and high-dimensional nature of the data. Indeed, this process not only requires spatial transformation, but also tensor reorientation to account for its rotational component [1]. The existing diffusion tensor registration algorithms can be subdivided in two classes. The first class of methods transforms the diffusion tensor data in multi-channel feature images and uses vector-data registration algorithms. For instance, in [2], both geometric features describing the distribution characteristics of tensor geometry over an isotropic neighborhood and orientation features based on principal directions distributions are combined for vector registration. Similarly, tensor shape and orientation are both taken into account in [3] using the Geodesic Loxodromes-based distance and a modified version of Multidimensional Scaling. The work in [4] investigated the use of multi-channel demons registration using the T2-weighted signal and tensor eigenvalues in a feature vector. In [5], several scalar values derived from diffusion tensors are studied for feature selection and tensor components provide better experimental performance. The method in [6] proposes a multi-resolution

scheme based on tensor-template matching through the extension of similarity measures from the scalar to the tensor case. The second class of approaches opts for the use of a metric for tensor matching in a framework previously used for standard image registration. For instance, the algorithm in [7] uses the symmetrized Kullback-Leibler divergence between probability distributions in the fluid registration framework, followed by a preservation of principal directions (PPD) tensor reorientation. The methods proposed in [8] and [9] use an explicit reorientation scheme in the registration framework. The former suggests an exact Finite-Strain (FS) differential and includes it in the demons algorithm, the latter proposes a piecewise affine deformation model and optimizes over the available rotational component of each affine transformation. It also provides an affine registration framework based on an L^2 distance between diffusion profiles.

1.3 Contributions of this Work

We note that in a DT registration context, it is important to combine spatial and diffusion information and not to treat them separately. Unlike the existing literature, we propose a method that combines simultaneously both tensor and spatial information in a probabilistic framework. By mapping implicitly the diffusion tensor images to a RKHS, we define local smoothness properties of the registration deformation to account both for the transformation regularity and for the reorientation of tensors. This mapping defines also a closed-form metric for tensor matching. Furthermore, we extend the framework proposed in [10] to diffusion tensor images by minimizing the defined energy in a discrete setting using the fast Primal-Dual (fast-PD) algorithm [11]. This is done by considering a quantized six-dimensional deformation space where the quaternion representation of rotations allows for proper interpolation and discrete sampling.

The remainder of this report is organized as follows: In section 2, the kernel over the tensor space is discussed while in the section 3, the concept of the proposed deformable registration framework is presented. Section 4 is dedicated to experimental results and the perspectives of this work are discussed in section 5.

2 Mapping Diffusion Probabilities to a Hilbert Space

Given the orientational nature of DT data, considering tensors independently from their particular spatial arrangement is a major drawback in a registration process. To overcome this issue, the spatial information can be incorporated in a probabilistic setting. Diffusion tensors measure the motion distribution of water molecules. More explicitly, they refer to the covariance of a Gaussian probability over the displacements $\mathbf{r}$ of the water protons given a diffusion (mixing) time t:

$$p(\mathbf{r}|t,\mathbf{D}) = \frac{1}{\sqrt{\det(\mathbf{D})(4\pi t)^3}} \exp\left(-\frac{\mathbf{r}^t\mathbf{D}^{-1}\mathbf{r}}{4t}\right) \tag{1}$$

Given a diffusion tensor $\mathbf{D}$ localized at voxel $\mathbf{x}$, we can obtain the probability of the position y of the water molecule previously localized at $\mathbf{x}$ in a straightforward way:

$$p(\mathbf{y}|\mathbf{x},t,\mathbf{D}) = \frac{1}{\sqrt{\det(\mathbf{D})(4\pi t)^3}} \exp(-\frac{(\mathbf{y}-\mathbf{x})^t\mathbf{D}^{-1}(\mathbf{y}-\mathbf{x})}{4t}) \tag{2}$$

Let us consider two probabilities p_1 and p_2 that model local Gaussian diffusion processes with diffusion tensors $\mathbf{D}_1$ and $\mathbf{D}_2$ at locations $\mathbf{x}_1$ and $\mathbf{x}_2$. We consider the normalized L^2 inner-product $k_t(p_1,p_2)$ between these probabilities:

$$k_t(p_1,p_2) = \frac{\int p_1\left(\mathbf{y}|\mathbf{x_1},t,\mathbf{D}_1\right) p_2\left(\mathbf{y}|\mathbf{x_2},t,\mathbf{D}_2\right) d\mathbf{y}}{\sqrt{\int \left(p_1\left(\mathbf{y}|\mathbf{x_1},t,\mathbf{D}_1\right)\right)^2 d\mathbf{y}}\sqrt{\int \left(p_2\left(\mathbf{y}|\mathbf{x_2},t,\mathbf{D}_2\right)\right)^2 d\mathbf{y}}} \tag{3}$$

It can be shown based on [**?**] that k_t has a closed-form expression:

$$k_t(p_1,p_2) = \underbrace{2\sqrt{2}\,\frac{\det(\mathbf{D}_1)^{\frac{1}{4}}\det(\mathbf{D}_2)^{\frac{1}{4}}}{\sqrt{\det(\mathbf{D}_1+\mathbf{D}_2)}}}_{\text{tensor similarity term}} \underbrace{\exp\left(-\frac{1}{4t}(\mathbf{x}_1-\mathbf{x}_2)^t(\mathbf{D}_1+\mathbf{D}_2)^{-1}(\mathbf{x}_1-\mathbf{x}_2)\right)}_{\text{spatial connectivity term}} \tag{4}$$

Note how this formulation allows for a simultaneous combination of spatial localization and diffusion tensor information and that t is a natural scale parameter. This is suitable for a better modeling of interactions between tensors. The kernel k_t verifies the Mercer property and therefore accounts for an implicit mapping ϕ from the space of Gaussian probabilities to a RKHS $\mathcal{H}$ endowed with an inner-product $< .,. >_{\mathcal{H}}$ such that $< \phi(p_1), \phi(p_2) >_{\mathcal{H}} = k_t(p_1,p_2)$. The normalized kernel k_t implies a Euclidean distance (L_2 norm) δ_t given by $\delta_t(p_1,p_2) = \sqrt{2-2k_t(p_1,p_2)}$. It is important to note that k_t and δ_t are invariant with respect to translational and rotational transformations. Indeed, when considering a translation vector $\mathbf{t}$ and a rotation matrix $\mathbf{R}$, this property can be verified easily by replacing $\mathbf{x}_1$ (resp. $\mathbf{x}_2$) by $\mathbf{R}\mathbf{x}_1+\mathbf{t}$ (resp. $\mathbf{R}\mathbf{x}_2+\mathbf{t}$) and $\mathbf{D}_1$ (resp. $\mathbf{D}_2$) by $\mathbf{R}\mathbf{D}_1\mathbf{R}^t$ (resp. $\mathbf{R}\mathbf{D}_2\mathbf{R}^t$) in (Eq.4). In order to ease the notation, in the remainder of the report we will identify a Gaussian probability distribution with its parameters and denote:

$$\delta_t(p_1(\mathbf{y}|\mathbf{x}_1,t,\mathbf{D}_1),p_2(\mathbf{y}|\mathbf{x}_2,t,\mathbf{D}_2)) = \delta_t((\mathbf{x}_1,\mathbf{D}_1),(\mathbf{x}_2,\mathbf{D}_2)) \tag{5}$$

3 Deformable Registration

Let us consider a source DT image $U : \Omega \mapsto S_+(3)$ and a target image V, where Ω is the source image domain and $S_+(3)$ is the space of symmetric positive definite matrices. We aim at computing a deformation field $\mathcal{T} : \Omega \mapsto \mathbb{R}^3 \times \mathrm{SO}(3)$ where SO(3) is the special orthogonal group. At each point $\mathbf{x} \in \Omega$, $\mathcal{T}(\mathbf{x}) = (\mathbf{t}(\mathbf{x}),\mathbf{R}(\mathbf{x}))$ is a pair composed of a translation vector $\mathbf{t}(\mathbf{x})$ and a rotation matrix $\mathbf{R}(\mathbf{x})$ that deforms U in an image W such that $W(\mathbf{x}+\mathbf{t}(\mathbf{x})) = \mathbf{R}(\mathbf{x})U(\mathbf{x})\mathbf{R}(\mathbf{x})^t$.

3.1 Deformation Model

We consider a grid-based deformation model that can provide for one-to-one and invertible transformations. The basic idea of the deformation model is that by superimposing a grid $G : [1, K] \times [1, L] \times [1, M]$ (where K, L and M are smaller than the dimensions of the domain) onto the moving image, it is possible to deform the embedded image by manipulating the control points belonging to the grid. Consequently, the goal is to recover the deformation vector $\mathcal{T}_{\mathbf{p}} = (\mathbf{t}_{\mathbf{p}}, \mathbf{R}_{\mathbf{p}})$ that should be applied to the node $\mathbf{p}$ of the grid, in order for the images to be aligned. In such a framework, the deformation $\mathcal{T}(\mathbf{x}) = (\mathbf{t}(\mathbf{x}), \mathbf{R}(\mathbf{x}))$ that should be applied to an image position $\mathbf{x}$ can be obtained through interpolation of the deformations obtained at the control points:

$$\mathbf{t}(\mathbf{x}) = \sum_{\mathbf{p} \in G} \eta_s(|\mathbf{x} - \mathbf{p}|)\mathbf{t}_{\mathbf{p}}, \quad \mathbf{R}(\mathbf{x}) = \sum_{\mathbf{p} \in G} \eta_r(|\mathbf{x} - \mathbf{p}|)\mathbf{R}_{\mathbf{p}}. \tag{6}$$

η_s and η_r are functions that weight the influence of each control point of the grid to each point of the domain in relation to their spatial distance from it. Note that the interpolation of rotations is not performed in SO(3) but in the quaternion space, i.e.

$$\mathbf{q}(\mathbf{x}) = \frac{\sum_{\mathbf{p} \in G} \eta_r(|\mathbf{x} - \mathbf{p}|)\mathbf{q}_{\mathbf{p}}}{\left\| \sum_{\mathbf{p} \in G} \eta_r(|\mathbf{x} - \mathbf{p}|)\mathbf{q}_{\mathbf{p}} \right\|}, \tag{7}$$

where $\mathbf{q}(\mathbf{x})$ (resp. $\mathbf{q}_{\mathbf{p}}$) is the quaternion representation of $\mathbf{R}(\mathbf{x})$ (resp. $\mathbf{R}_{\mathbf{p}}$). The matrix representation $\mathbf{R}(\mathbf{x})$ is then obtained easily from $\mathbf{q}(\mathbf{x})$.

3.2 DT Image Registration: Continuous Domain

Given the above-defined deformation model, the DT images will be deformed in such a way that an appropriately defined dissimilarity criterion with respect to the distance δ_t implied by the kernel k_t is minimized:

$$E_{data} = \int_{\Omega} \delta_t((\mathbf{x}, W(\mathbf{x})), (\mathbf{x}, V(\mathbf{x})))d\mathbf{x}. \tag{8}$$

E_{data} is simply a data term that will drive the deformation towards a minimal mismatch between the deformed image W and the target image V. Note that in E_{data}, only the tensor similarity term in (Eq.4) is relevant, since we will compare tensors that share the same location. We can rewrite E_{data} using the the control points of the superimposed grid G. Indeed, each voxel $\mathbf{x}$ is back-projected to the points of the grid, in the following form:

$$E_{data} = \frac{1}{|G|} \sum_{\mathbf{p} \in G} \int_{\Omega} \eta_p^{-1}(|\mathbf{x} - \mathbf{p}|)\delta_t((\mathbf{x}, W(\mathbf{x})), (\mathbf{x}, V(\mathbf{x})))d\mathbf{x}. \tag{9}$$

The back-projection function η^{-1} computes the influence of the position $\mathbf{x}$ to the control point $\mathbf{p}$. If the nearest neighbor weighting scheme is considered, then each position $\mathbf{x}$

contributes to only one control point $\mathbf{p}$ with a weight equal to one. In the general case, it takes the following form

$$\eta_p^{-1} = \frac{\eta_p(|\mathbf{x}-\mathbf{p}|)}{\int_\Omega \eta_p(|\mathbf{x}-\mathbf{p}|)}. \tag{10}$$

It should be noted that, as the different indices imply, different weighting schemes can be used for the interpolation of the displacement field (η_s), the interpolation of the rotations (η_r) as well as for the back-projection to the nodes of the grid (η_p).

The minimization of E_{data} is ill-posed as there are fewer constraints than the number of variables to be determined. A common way to tackle such a limitation is to consider a regularization term that will smooth the deformation field, and more importantly take into account local structural information of the source image U. We suppose that the deformation field will be approximately, up to a suitable change in the diffusion time t to account for local scale, *locally isometric*, i.e. that it preserves the distance δ_t between spatially neighboring Gaussian probabilities when deforming U. This leads us to define the following smoothness term:

$$E_{smooth} = \int_\Omega \int_{\mathbf{z}\in\mathcal{N}_\mathbf{x}} |\delta_t((\mathbf{x},U(\mathbf{x})),(\mathbf{z},U(\mathbf{z}))) - \delta_{t_{\mathbf{xz}}}((\overline{\mathbf{x}},W(\overline{\mathbf{x}})),(\overline{\mathbf{z}},W(\overline{\mathbf{z}})))|\, d\mathbf{z}d\mathbf{x} \tag{11}$$

where $\overline{\mathbf{x}} = \mathbf{x} + \mathbf{t}(\mathbf{x})$, $\overline{\mathbf{z}} = \mathbf{z} + \mathbf{t}(\mathbf{z})$, $t_{\mathbf{xz}} = t\frac{||\overline{\mathbf{x}}-\overline{\mathbf{z}}||}{||\mathbf{x}-\mathbf{z}||}$ and $\mathcal{N}_\mathbf{x}$ is a local neighborhood of $\mathbf{x}$. We expect the minimization of E_{smooth} to favor tensor reorientation so that the local source image structure can be preserved in the deformed image. The energy can be defined over the control points of the grid G instead of the entire source domain Ω by considering a neighborhood structure on G. In order to recover the optimal deformation parameters, we have to minimize the registration energy

$$E = E_{data} + \alpha E_{smooth}, \tag{12}$$

where α is a trade-off factor.

A natural way to continue would be to apply a gradient-descent optimization scheme. Such an approach has certain advantages, it is intuitively simple and easy to implement, though it suffers from some important disadvantages. It is prone to stuck in local minima and it is not modular as it depends both on the deformation model used and the objective criterion to be minimized. Moreover, it is computationally demanding. Ideally, one would prefer a method that would be able to provide a solution in an efficient way and at the same time guarantee that it will be "close" to the optimal one. Methods that comply with the previous characteristics can be found in the discrete optimization field.

Following recent ideas in scalar image registration [10] and recent advances in discrete optimization [11], we opt for the use of a discrete optimization technique called Fast-PD [11]. The advantages of the Fast-PD consist in its ability to provide an optimal solution (up to a user-defined bound) in an efficient way. Moreover, it allows for a gradient-free optimization thus permitting the use of different deformation methods. In the following, we detail the discretization of the deformation space as well as the Markov Random Field (MRF) formulation of the problem.

3.3 DT Image Registration: Discrete Domain

To be able to apply the Fast-PD optimization, it is obligatory to provide a quantized version of the deformation space. Let $\Theta = (\mathbf{d}^1, \ldots, \mathbf{d}^n)$ be a quantized version of the deformation space $\mathbb{R}^3 \times \mathrm{SO}(3)$, then to each quantized deformation $\mathbf{d}^i$, a label l^i can be assigned to it, thus defining a discrete set of labels $L = \{l^1, \ldots, l^n\}$. Then, assigning a label $l_\mathbf{p}$ to the node $\mathbf{p}$, where $l_\mathbf{p} \in L$, corresponds to applying the deformation $\mathbf{d}^{l_\mathbf{p}}$ to the node, that is translating it by $\mathbf{t}^{l_\mathbf{p}}$ and rotating the corresponding tensor by $\mathbf{R}^{l_\mathbf{p}}$. The quantization of spatial displacements is intuitive , the case of rotations is however less straightforward. In order to quantize the group of rotation matrices, we use their quaternion representation. The problem is equivalent to sampling points over the unit sphere $\mathbb{S}^3$ of $\mathbb{R}^4$. We use layered Sukharev Grid sequences [12] that offer a multi-resolution, deterministic and uniform sampling of $\mathbb{S}^3$ by back-projecting points sampled over a hypercube inscribed in $\mathbb{S}^3$ outward onto the spherical surface. The set Θ is therefore formed by the pairs of sampled translations and rotations.

Following [10], we cast the registration problem as a discrete multi-labeling problem. In such a context, the goal is to recover the optimal individual label $l_\mathbf{p}$ that should be assigned to each node $\mathbf{p}$ of the grid. This can be done using the theory of MRFs, the general form of which is the following:

$$E_{\mathrm{MRF}} = \sum_{\mathbf{p} \in G} V_\mathbf{p}(l_\mathbf{p}) + \alpha \sum_{\mathbf{p} \in G} \sum_{\mathbf{q} \in \mathcal{N}(\mathbf{p})} V_{\mathbf{pq}}(l_\mathbf{p}, l_\mathbf{q}) \tag{13}$$

where $V_\mathbf{p}(\cdot)$ are the unary potentials that encode the data term and $V_{\mathbf{pq}}(\cdot,\cdot)$ are the pairwise potentials that encode smoothness constraints. $\mathcal{N}(\mathbf{p})$ represents the neighborhood system of the node $\mathbf{p}$. The unary potentials will be defined according to the data term in Eq.8:

$$V_\mathbf{p} \approx \int_\Omega \eta_p^{-1}(|\mathbf{x} - \mathbf{p}|)\delta_t((\mathbf{x}, W(\mathbf{x})), (\mathbf{x}, V(\mathbf{x})))d\mathbf{x}. \tag{14}$$

Similarly the pairwise potentials are derived following (Eq.11):

$$V_{\mathbf{pq}}(l_\mathbf{p}, l_\mathbf{q}) = \left|\delta_t((\mathbf{p}, U(\mathbf{p})), (\mathbf{q}, U(\mathbf{q}))) - \delta_{t_{\mathbf{pq}}}((\overline{\mathbf{p}}, W(\overline{\mathbf{p}})), (\overline{\mathbf{q}}, W(\overline{\mathbf{q}})))\right| \tag{15}$$

where $(\overline{\mathbf{p}}, W(\overline{\mathbf{p}}))$ (resp. $(\overline{\mathbf{q}}, W(\overline{\mathbf{q}}))$) are obtained by applying the deformation parameters of the label $l_\mathbf{p}$ (resp. $l_\mathbf{q}$).

The main challenge of discrete optimization methods is the quantization of the search space. When quantizing the deformation space a compromise between the computational complexity and the ability to capture a good minimum is sought. A great number of labels will permit us to be confident that the optimal solution will be approached but will result in high computational times and great memory demands. On the other hand, a small number of labels will keep the computational time small but will, in general, fail to approach the optimal solution with precision. A compromise can be achieved through a compositional approach, where the final solution is obtained through successive optimization problems [13, 10]. In each successive optimization problem finer grids (and consequently shorter

diffusion times t) and label sets will be applied. Thus, by keeping the set of the labels in a reasonable size it becomes possible to approximate the optimal solution in an efficient way.

4 Experimental Validation

For validation purposes, we considered DT images of the calf muscle of 10 healthy subjects. The images were acquired with a 1.5 T MRI scanner using the following parameters : repetition time (TR)= 3600 ms, echo time(TE) = 70 ms, slice thickness = 7 mm and b value of 700 $s.mm^{-2}$ with 12 gradient directions and 13 repetitions. The size of the obtained volumes is $64 \times 64 \times 20$ voxels with a voxel resolution of $3.125mm \times 3.125mm \times 7mm$. High-resolution T1-weighted images were simultaneously acquired and segmented in 7 muscle groups by an expert. In order to assess quantitatively our method, we consider several evaluation criteria. In order to measure the spatial mismatch between the deformed and the target images, we deform the ground-truth segmentations and compute the dice overlap, the sensitivity and the specificity of the deformed source segmentation with respect to the target segmentation. Four angular similarity criteria are also evaluated on the target mask: the mean difference in the azimuthal angle θ and the polar angle ϕ in spherical coordinates of the principal directions of diffusion, their average angular separation (AAS) as well as the average overlap of eigenvalue-eigenvector pairs (AOE). We also compute the mean difference in fractional anisotropy (FA).

Among the possible 90 registrations, we chose randomly a subset of 50 pairs of DT images. In all our experiments, we used a three-level multiresolution scheme. The grids used at the three levels were of size $6 \times 6 \times 5$, $12 \times 12 \times 10$ and $18 \times 18 \times 15$. The following diffusion times were used: $t = \left\{2\ 10^5, 5\ 10^4, 2\ 10^4\right\}$. The parameter α in (Eq.13) was set to $\alpha = 1$. A number of $73 = 18 \times 4 + 1$ translation labels were used per resolution level, sampled along the horizontal and vertical directions as well as the diagonals. For rotation sampling, we generated 10^3, 10^4 and 10^5 quaternions using Sukharev layered grids. Of these we selected 100, 50 and 25 for the three levels respectively. These samples were chosen as the closest with respect to the geodesic distance $\arccos(.,.)$ on $\mathbb{S}^3$ to the identity matrix (or equivalently with the smallest angle). Towards imposing the diffeomorphic property on the deformation field, we use a cubic B-spline interpolation of the displacement field, with the maximum displacement being restricted to 0.4 times the grid spacing. We used a simple trilinear scheme for tensor interpolation and a nearest-neighbor backprojection (η_p). For the sake of comparison, we provide the values of the computed evaluation criteria before and after registration. We also compare our method to a reference algorithm recently proposed in [8] (the software is publicly available at `http://www-sop.inria.fr/asclepios/software/MedINRIA/`) and to the result of our method without a rotational component, i.e. with a single rotation label equal to the identity matrix. For the reference algorithm, we considered a three-level multiresolution pyramid with a smoothing kernel of size 1 and a maximum displacement of 4. We report in (Fig.2) the boxplots of the evaluation criteria over the 50 registrations for our method and for the approaches described above. We can see from the boxplots that our approach improves significantly all the evaluation criteria with respect to

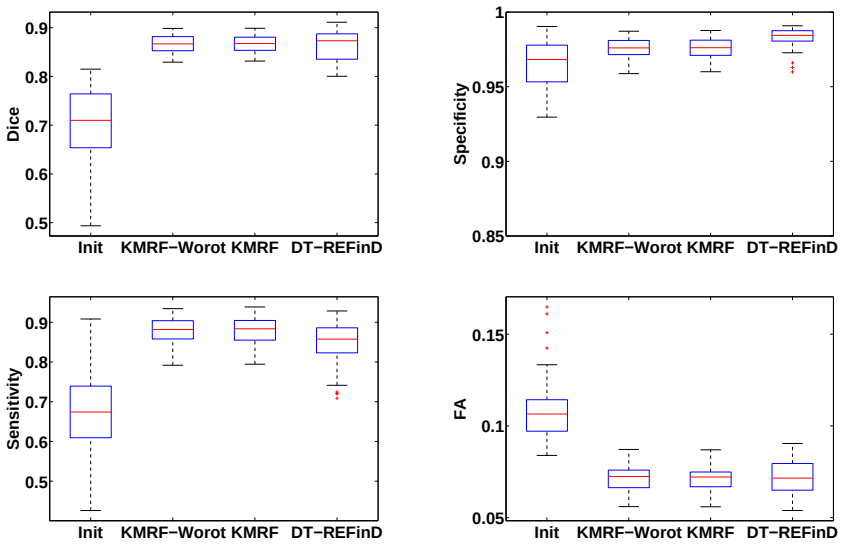

Figure 1: Boxplots of the evaluation criteria over the 50 registrations before registration (Init), with our method with a single identity rotation label (KMRF-Worot) and several rotation labels (KMRF), as well as the method in [8] (DT-REFinD).

the initial state (no registration) and that it achieves close results to [8]. We run a paired statistical Student t-test with a significance level of 0.05 for comparison and we found that the two approaches performed equivalently for the dice and FA, that our method achieved better results for θ, AAS and sensitivity while [8] performed better in ϕ, AOE and specificity. The inclusion of rotation labels improved (in a significant way according to the t-test) all the four angular evaluation criteria with respect to the no-rotation experiments. For qualitative evaluation, we report in (Fig.3) a view of moving tensors, target tensors and deformed tensors, all overlaid on the B0-image of the target subject. We can see that the spatial mismatch is minimized while the tensor field obtained is smooth and the directions of the deformed tensors are similar to the fixed ones. The algorithm runs in approximately 15 minutes on a standard PC.

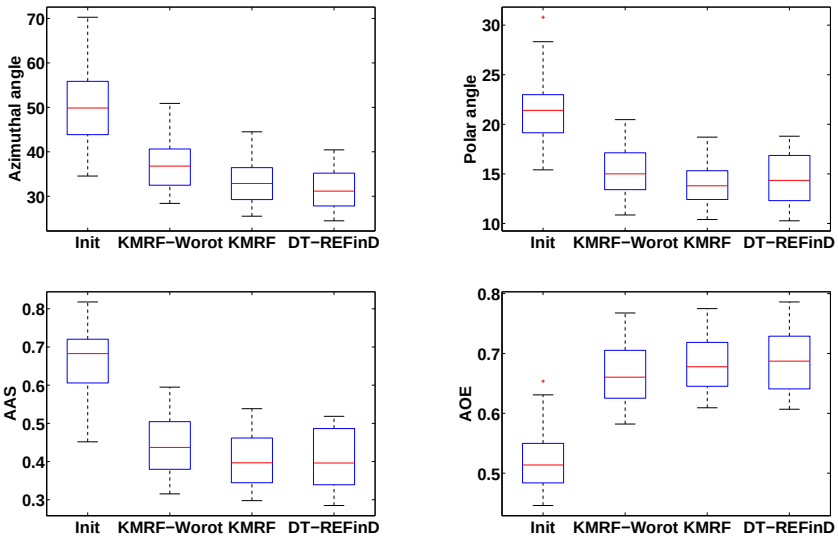

Figure 2: Boxplots of the evaluation criteria over the 50 registrations before registration (Init), with our method with a single identity rotation label (KMRF-Worot) and several rotation labels (KMRF), as well as the method in [8] (DT-REFinD).

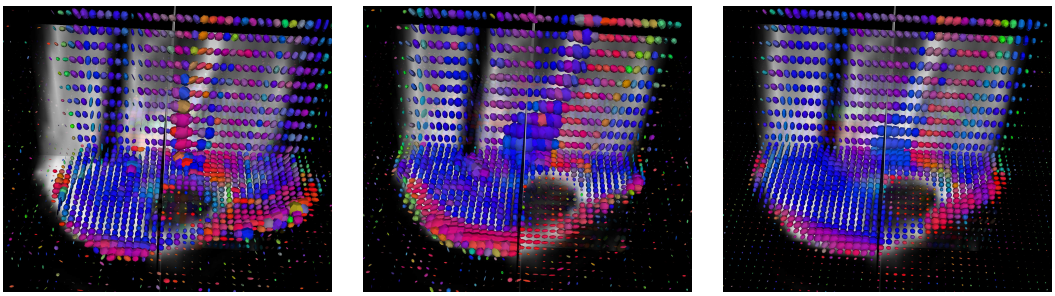

Figure 3: From left to right: moving, fixed and deformed tensors. All are overlaid on the B0-image of the target subject. RGB colors encode principal directions of diffusion.

5 Conclusion

6 Discussion

We introduced a novel approach to diffusion tensor registration. The main contribution is two-fold, on one hand we proposed to use a diffusion probability kernel that models both spatial and data dependencies in the tensor field in order to drive the registration process. The proposed formulation allows for the matching of the deformed and the target images while reorienting the tensors and taking into account the local structural information of the source image. On the other hand, we showed that the discrete MRF-based formulation for scalar images proposed in [10] can also be extended to the case of tensor images. A possible improvement of the proposed framework is to consider automatic and location-dependent adaptive quantization of the search space in the context of discrete optimization. This could improve significantly the performance of the method especially when seeking an adequate discretization of such high-dimensional spaces.

References

[1] D. C. Alexander, C. Pierpaoli, P. J. Basser, and J. C. Gee, "Spatial transformations of diffusion tensor magnetic resonance images.," *IEEE TMI*, vol. 20, no. 11, pp. 1131–1139, 2001.

[2] Jinzhong Yang, Dinggang Shen, Christos Davatzikos, and Ragini Verma, "Diffusion tensor image registration using tensor geometry and orientation features," in *MICCAI*, 2008.

[3] M. Okan Irfanoglu, Raghu Machiraju, Steffen Sammet, Carlo Pierpaoli, and Michael V. Knopp, "Automatic deformable diffusion tensor registration for fiber population analysis," in *MICCAI*, 2008.

[4] A. Guimond, C. R. G. Guttmann, S. K. Warfield, and C.-F. Westin, "Deformable registration of DT-MRI data based on transformation invariant tensor characteristics," in *ISBI*, 2002.

[5] H. J. Park, M. Kubicki, M. E. Shenton, A. Guimond, R. W. McCarley, S. E. Maier, R. Kikinis, F. A. Jolesz, and C.-F. Westin, "Spatial normalization of diffusion tensor MRI using multiple channels," *Neuroimage*, vol. 20, no. 4, pp. 1995–2009, 2003.

[6] J. Ruiz-Alzola, C.-F. Westin, S. K. Warfield, C. Alberola, S. E. Maier, and R. Kikinis, "Nonrigid registration of 3d tensor medical data," *Medical Image Analysis*, vol. 6, no. 2, pp. 143–161, 2002.

[7] Ming-Chang Chiang, Alex D. Leow, Andrea D. Klunder, Rebecca A. Dutton, Marina Barysheva, Stephen E. Rose, Katie McMahon, Greig I. de Zubicaray, Arthur W. Toga, and Paul M. Thompson, "Fluid registration of diffusion tensor images using information theory.," *IEEE TMI*, vol. 27, no. 4, pp. 442–456, 2008.

[8] B. Yeo, T. Vercauteren, P. Fillard, X. Pennec, P. Golland, N. Ayache, and O. Clatz, "DTI registration with exact finite-strain differential," in *ISBI*, 2008.

[9] Hui Zhang, Paul A. Yushkevich, Daniel C. Alexander, and James C. Gee, "Deformable registration of diffusion tensor MR images with explicit orientation optimization," *Medical Image Analysis*, vol. 10, no. 5, pp. 764 – 785, 2006.

[10] B. Glocker, N. Komodakis, G. Tziritas, N. Navab, and N. Paragios, "Dense image registration through MRFs and efficient linear programming," *Medical Image Analysis*, vol. 12, no. 6, pp. 731–741, 2008.

[11] N. Komodakis, G. Tziritas, and N. Paragios, "Performance vs computational efficiency for optimizing single and dynamic mrfs: Setting the state of the art with primal-dual strategies," *CVIU*, 2008.

[12] Anna Yershova and Steven M. LaValle, "Deterministic sampling methods for spheres and SO(3)," in *ICRA*, 2004.

[13] O. Veksler, *Efficient graph-based energy minimization methods in computer vision*, Ph.D. thesis, Cornell University, 1999.

Unité de recherche INRIA Futurs
Parc Club Orsay Université - ZAC des Vignes
4, rue Jacques Monod - 91893 ORSAY Cedex (France)

Unité de recherche INRIA Lorraine : LORIA, Technopôle de Nancy-Brabois - Campus scientifique
615, rue du Jardin Botanique - BP 101 - 54602 Villers-lès-Nancy Cedex (France)
Unité de recherche INRIA Rennes : IRISA, Campus universitaire de Beaulieu - 35042 Rennes Cedex (France)
Unité de recherche INRIA Rhône-Alpes : 655, avenue de l'Europe - 38334 Montbonnot Saint-Ismier (France)
Unité de recherche INRIA Rocquencourt : Domaine de Voluceau - Rocquencourt - BP 105 - 78153 Le Chesnay Cedex (France)
Unité de recherche INRIA Sophia Antipolis : 2004, route des Lucioles - BP 93 - 06902 Sophia Antipolis Cedex (France)

Éditeur
INRIA - Domaine de Voluceau - Rocquencourt, BP 105 - 78153 Le Chesnay Cedex (France)
http://www.inria.fr
ISSN 0249-6399